



Published in final edited form as:

Chem Res Toxicol. 2020 June 15; 33(6): 1328–1338. doi:10.1021/acs.chemrestox.9b00255.

Atropselective Disposition of 2,2',3,4',6-Pentachlorobiphenyl (PCB 91) and Identification of Its Metabolites in Mice with Liver-specific Deletion of Cytochrome P450 Reductase

Xianai Wu[†], Guangshu Zhai^{‡,§}, Jerald L. Schnoor^{†,‡,§}, Hans-Joachim Lehmler^{†,§}

[†]Department of Occupational and Environmental Health, The University of Iowa, Iowa City, IA, 52242, USA

[‡]Department of Civil and Environmental Engineering, The University of Iowa, Iowa City, IA, 52242, USA

[§]IHR Hydrosience and Engineering, The University of Iowa, Iowa City, IA, 52242, USA

Abstract

Hepatic cytochrome P450 enzymes metabolize chiral polychlorinated biphenyls (PCBs) to hydroxylated metabolites (OH-PCBs). Animal models with impaired metabolism of PCBs are one approach to study how the atropselective oxidation of PCBs to OH-PCBs contributes to toxic outcomes, such as neurodevelopmental disorders, following PCB exposure. We investigated the disposition of PCB 91, a *para*-substituted PCB congener, in mice with a liver-specific deletion of the cytochrome P450 reductase (*cpr*) gene (KO mice). KO mice and wild type (WT) mice were exposed orally to racemic PCB 91 (30 mg/kg b.w.). Levels and enantiomeric fractions of PCB 91 and its hydroxylated metabolites were determined in tissues three days after PCB exposure and in excreta on days 1 to 3 after PCB exposure. PCB 91, but not OH-PCB levels were higher in KO compared to WT mice. The elevated fat and protein content in the liver of KO mice resulted in the hepatic accumulation of PCB 91. OH-PCBs were detected in blood, liver, and excreta samples of KO and WT mice. 2,2',3,4',6-Pentachlorobiphenyl-5-ol (5-91) was the major metabolite. A considerable percent of the total PCB 91 dose (%TD) was excreted with the feces as 5-91 (23 %TD and 31 %TD in KO and WT mice, respectively). We tentatively identified glucuronide and sulfate metabolites present in urine samples. The PCB 91 atropisomer eluting first on the chiral column (E₁-PCB 91) displayed genotype-dependent atropisomeric enrichment, with a more pronounced atropisomeric enrichment observed in WT compared to KO mice. E₁-atropisomers of 5-91 and 2,2',3,4',6-pentachlorobiphenyl-4-ol (4-91) were enriched in blood and liver, irrespective of the genotype; however, the extent of the enrichment of E₁-5-91 was genotype-dependent. These differences in atropselective disposition are consistent with slower metabolism

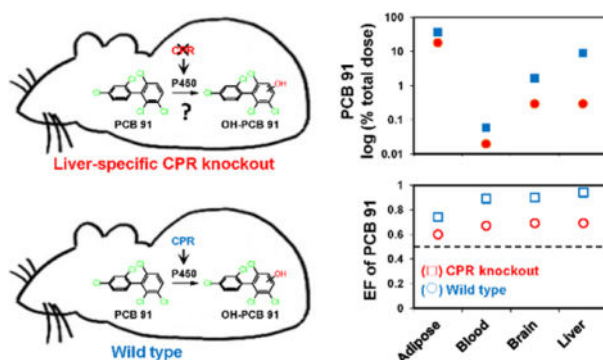
Corresponding Author: Dr. Hans-Joachim Lehmler, The University of Iowa, Department of Occupational and Environmental Health, University of Iowa Research Park, B164 MTF, Iowa City, IA 52242-5000, Phone: (319) 335-4981, Fax: (319) 335-4290, hans-joachim-lehmler@uiowa.edu.

SUPPORTING INFORMATION AVAILABLE

The supporting information includes a characterization of the mouse model, including body and organ weights; wet weight and lipid-adjusted concentrations of PCB 91 and its metabolites; amount of PCB 91 and its metabolites expressed as percent of the total PCB 91 dose; comparison of the enantiomeric fraction of the PCB 91, 5-91 and 4-91; limits of detection (*LODs*) and background levels of PCB 91 and its metabolites; and extractable lipid content in tissues and excreta WT and KO mice. This material is available free of charge via the Internet at <http://pubs.acs.org>.

of PCB 91 in KO compared to WT mice and the accumulation of the parent PCB in the fatty liver of KO mice.

Graphical Abstract



INTRODUCTION

PCBs were produced and used as complex mixtures containing many structurally diverse PCB congeners, including PCB 91. In the United States, technical PCB mixtures were sold under the tradename Aroclor. These mixtures contain anywhere from zero to one percent by weight of PCB 91. Approximately 1,000 metric tons of this PCB congener were produced globally.¹ The production of PCBs was banned in the United States in the late 1970s due to environmental and human health concerns. However, PCBs are inadvertent byproducts of industrial processes and, as a result, can still be found in consumer products, including paint pigments^{2, 3} and polymer resins.⁴ PCBs persist in the environment because of their resistance to chemical and thermal degradation, and bioaccumulate and biomagnify in aquatic and terrestrial food chains. Because cytochrome P450 enzymes readily metabolize lower chlorinated PCB congeners to OH-PCBs,^{1, 5, 6} these PCB congeners have low detection frequencies in human biomonitoring studies; however, humans are continuously exposed to these congeners.

Epidemiological and animal studies implicate exposure to PCBs in a range of adverse health outcomes, including neurodevelopmental disorders.⁷ In particular, PCB congeners with several *ortho* chlorine substituents are sensitizers of ryanodine receptors (RyRs),^{8, 9} intracellular calcium channels implicated in PCB-induced developmental neurotoxicity.¹⁰ Other proposed mechanisms of PCB neurotoxicity include altered neurotransmitter and calcium homeostasis, oxidative stress, and effects on the thyroid hormone system.^{11, 12} A recent study demonstrates that PCBs' effects on RyRs, but not the thyroid hormone receptor are drivers of adverse neurodevelopmental outcomes following PCB exposure.¹³ There is also evidence that PCB metabolites, in particular OH-PCBs, are toxic to the developing brain. OH-PCBs are potent sensitizers of RyRs^{9, 14} and can be present in the rodent brain.^{15, 16} Moreover, animal studies reveal adverse neurobehavioral outcomes following developmental exposure to OH-PCBs.^{17, 18}

The oxidation of PCBs by cytochrome P450 enzymes forms OH-PCBs. PCB congeners without *para* chlorine substituents are more readily metabolized than PCB congeners with a *para* substituent. PCB 91, a PCB congener with a *para* chlorine substituent, is preferentially oxidized to a 1,2-shift metabolite with the hydroxy group in the *meta* position by human liver microsomes.^{19, 20} Compared to PCB 91, distinctively different metabolite profiles are observed from PCB 95 (2,2',3,5',6-pentachlorobiphenyl) and PCB 136 (2,2',3,3',6,6'-hexachlorobiphenyl), PCB congeners without a *para* chlorine substituent, in metabolism studies with human liver microsomes.^{19, 21–23} In rodents, CYP2B enzymes play an important role in the metabolism of neurotoxic PCBs to *meta* hydroxylated OH-PCBs.^{1, 24} A considerable percent of the total dose of PCB 136 is excreted as a *meta* hydroxylated metabolite with the feces of PCB exposed mice.²⁵ These studies typically employed liver microsomes or liver tissue slices obtained from animals pretreated with phenobarbital, an inducer of hepatic CYP2B enzymes. Until now, the disposition of OH-PCBs in rodents and humans exposed to structurally diverse, *ortho* chlorinated PCBs (e.g., PCB 91) has received little attention.

PCB 91, like several other RyR-active PCBs and OH-PCBs, displays axial chirality. The presence of three or four *ortho* chlorine substituents hinders the rotation around the phenyl-phenyl bond. Consequently, PCB 91 and its metabolites exist as two rotational isomers, or atropisomers, that are non-superimposable mirror images of each other. The atropselective metabolism of chiral PCBs results in an atropisomeric enrichment of the parent PCBs and their metabolites.^{1, 26} This enrichment has toxicological implications because atropisomers can display different biological effects. For example, several studies have demonstrated atropselective effects of PCB 95 and PCB 136 atropisomers on RyRs and neuronal connectivity in primary neurons,^{27–29} endpoints implicated in PCB developmental neurotoxicity. It is likely that the atropisomers of OH-PCBs and other PCB metabolites also display atropselective toxicities; however, this hypothesis has not been investigated to-date.

Overall, the available evidence demonstrates that PCB and OH-PCBs atropisomers are present in the developing brain and affect cellular targets implicated in PCB developmental neurotoxicity, most likely in an atropselective manner. Therefore, it is important to assess how the atropselective oxidation of PCBs to OH-PCB metabolites contributes to neurotoxic outcomes on PCB exposed rodents and humans. The use of transgenic animal models with impaired hepatic metabolism of PCBs is one possible approach to address this question. Here, we investigate the atropselective disposition of PCB 91 in a well-established mouse model with a liver-specific deletion of the *cpr* gene (KO mice).^{30, 31} Our findings reveal genotype-dependent differences in the disposition of PCB 91 and its metabolites resulting from an impaired hepatic metabolism and the higher fat content in the liver and feces of KO compared to congenic WT mice.

EXPERIMENTAL SECTION

Analytical standards.

2,3,4',5,6-Pentachlorobiphenyl (PCB 117), 2,2',3,4,4',5,6,6'-octachlorobiphenyl (PCB 204) and 2,3,3',4,5,5'-hexachlorobiphenyl-4'-ol (4'-159) were obtained from AccuStandard (New Haven, CT, USA). PCB 91 and the corresponding OH-PCB metabolites were

synthesized as described earlier.³² The chemical structures and abbreviations of the PCB 91 metabolites are shown in Figure 1. Diazomethane was synthesized as a solution in diethyl ether from *N*-methyl-*N*-nitroso-*p*-toluenesulfonamide (Diazald) with an Aldrich mini Diazald apparatus (Milwaukee, WI, USA).

Animals.

The Institutional Animal Care and Use Committee of the University of Iowa approved all animal procedures (protocol #: 1206120). Alb-Cre^{+/-}/Cpr^{lox+/-} mice with a liver-specific deletion of the cytochrome P450 oxidoreductase gene (KO mice) and Alb-Cre^{-/-}/Cpr^{lox+/-} mice (WT mice) were obtained from Dr. Xinxin Ding (School of Public Health, State University of New York, Albany, NY). Mice were maintained as described in the Supporting Information (also, see references^{30, 31}). To study the disposition of racemic PCB 91, female KO and WT mice (age 12 to 13 weeks; Table S1) were randomly divided into treatment and control groups. WT (n=3) and KO (n=4) mice received a single oral dose PCB 91 (30 mg/kg b.w.) on a Vanilla Wafer cookie (7.5 g/kg b.w.). WT (n=2) and KO (n=2) control groups received the vehicle (Vanilla Wafer cookie; 7.5 g/kg b.w.) alone and were used to assess potential background contamination with PCB 91 and its metabolites. A detailed description of the preparation of the cookies for this dosing approach has been reported previously.³³ This route of administration was selected to reduce the stress of the animal. Moreover, the experimental design (i.e., sex, dose, and dosing period) was selected to facilitate a comparison with similar disposition studies in mice,^{25, 33-36} and to lay the groundwork for future studies of the developmental neurotoxicity in this mouse model.

After eating the entire cookie, animals were transferred to metabolic cages, and urine and feces were collected daily for three days. The two KO mice exposed to vehicle were housed together. All other mice were housed individually. Mice were euthanized by carbon dioxide asphyxiation followed by cervical dislocation three days after PCB 91 administration. Blood and tissues (brain, liver, and adipose tissue) were collected, and their wet weights were determined (Table S1). All samples were stored at -80 °C until further analysis. A discussion of phenotypes of KO vs. WT mice is provided in the Supporting Information.

Extraction of PCB 91 and its hydroxylated metabolites from tissue and blood samples.

PCB 91 and its metabolites were extracted by pressurized liquid extraction from liver (0.57–0.93 g), brain (0.18–0.30 g), adipose (0.06–0.34 g), and feces samples (0.29–0.35g) using a Dionex ASE200 system (Dionex, Sunnyvale, CA).³³ Briefly, the tissues were mixed with diatomaceous earth (2 g; Dionex) and placed in the extraction cell (33 mL) containing Florisil (60~100 mesh, 12 g; Fisher Scientific). PCB 117 (500 ng) and 4'-159 (137 ng) were added to each sample as surrogate recovery standards, and the cells were extracted with hexane-dichloromethane-methanol (48:43:9, v/v/v) at 100 °C and 1500 psi (10 MPa) with pre-heat equilibration for 6 min, 60% of cell flush volume, and 1 static cycle of 5 min.^{37, 38} Sample blanks containing only Florisil and diatomaceous earth were extracted in parallel with each sample set. The extracts were concentrated to approximately 1 mL using a Turbo Vap® II (Biotage, NC, USA) and transferred with hexane to glass tubes. The samples were evaporated to dryness under a gentle stream of nitrogen and redissolved in 1 mL of hexane. After derivatization of the OH-PCBs with a solution of diazomethane in diethyl ether, the

organic extracts were subjected to a sulfur clean-up step, followed by treatment with concentrated sulfuric acid as described earlier.³³

PCB 91 and its hydroxylated metabolites were extracted from blood samples (0.49 to 0.87 g) by liquid-liquid extraction following a published method.³⁷ Briefly, blood samples were diluted by 3 mL of 1% KCl and the surrogate recovery standards (PCB 117, 250 ng; 4'-159, 69 ng) were added. Each sample was acidified with 1 mL of 6 M HCl, followed by addition of 3 mL 2-propanol and 5 mL hexane: MTBE (1:1, v/v). After thoroughly mixing and centrifugation, the organic phase was transferred to the second tube, and each sample was extracted a second time with 3 mL of hexane. The combined organic phases were washed with 3 mL of KCl (1%). The samples were evaporated to dryness, derivatized with diazomethane, and further treated as described above for tissue samples.

β -Glucuronidase/sulfatase deconjugation of urine samples.

Two aliquots of each urine sample (approximately 0.1 to 0.6 mL) were diluted with an equal volume of 0.2 M sodium acetate buffer (pH=5) to determine if glucuronide or sulfate conjugates of hydroxylated PCB 91 metabolites were present in urine samples. Both aliquots were incubated in parallel with or without β -glucuronidase/sulfatase mixture (20 μ L; type H-2 from *Helix pomatia*, 100,000 units/mL; Sigma-Aldrich Co. St. Louis, MO, USA) for 12 h at 37 °C.²⁵ Subsequently, PCB 91 and its hydroxylated metabolites were extracted from urine samples as described above for blood.

Gas chromatographic analysis of PCB 91 and its metabolites.

PCB 91 and the methylated derivatives of hydroxylated PCB 91 metabolites were quantified either on a DB1-MS (60 m length, 250 μ m inner diameter, 0.25 μ m film thickness; Agilent, Santa Clara, CA) or an Equity-1 capillary column (60 m length, 250 μ m inner diameter, 0.25 μ m film thickness; Supelco, Bellefonte, PA) using an Agilent 7890A gas chromatograph equipped with two ⁶³Ni-micro electron capture detectors (μ ECD).³⁹ The levels of PCB and its metabolites were calculated using PCB 204 as internal standard (or volume corrector) and adjusted for tissue wet weight, lipid content or expressed as %TD (Tables S2–S6). If not stated otherwise, tissue levels are reported as %TD throughout the manuscript. The same trends in tissue levels were observed when levels were adjusted for tissue wet weight or extractable lipid content.

Enantiomeric fractions, a measure of the atropisomeric enrichment of PCB 91 and its metabolites, were determined on the same instrument described above.⁴⁰ PCB 91, 4-91 and 5-91 atropisomers were separated using a ChiralDex BDM (BDM) column (30 m length, 250 μ m inner diameter, 0.12 μ m film thickness; Supelco, St. Louis, MO). The atropisomers of PCB 91 and 5-91 were separated on CP-ChiraSil-DEX CB (CD) column (30 m length, 250 μ m inner diameter, 0.12 μ m film thickness; Agilent Technologies, Santa Clara, CA). The temperature program for the atropselective analyses was as follows: 10 °C/min from 100 to 140 °C, hold for 535 min, 10 °C/min to 200 °C, and hold for 15 min. Atropisomers of 4,5-91 (2,2',3,4',6-pentachlorobiphenyl-4,5-diol) did not resolve on either atropselective column. As described previously, the elution order of PCB 91 atropisomers are inverted on the BDM and CD column (i.e., E₁-PCB 91 on the BDM column and E₂-PCB 91 on the CD

column are the same PCB 91 atropisomer; vice versa, E₂-PCB 91 on the BDM column and E₁-PCB 91 on the CD column are the same PCB 91 atropisomer).⁴¹ If not stated otherwise, PCB 91 atropisomers are identified based on the elution order on the BDM column. The enantiomeric fraction (EF) values of PCB 91, 4-91, and 5-91 were determined as $EF = \text{Area } E_{(1)} / (\text{Area } E_{(1)} + \text{Area } E_{(2)})$ and are summarized in Table S7. For information regarding the quality assurance/quality control of the chemical analyses, including background levels of in tissues and excreta from control animals, see the Supporting Information and Tables S8 and S9.

Extractable lipid content.

Lipids were extracted from tissues and feces samples by pressurized liquid extraction as described earlier.³³ Briefly, the samples were mixed with 2 g of diatomaceous earth and placed in 11 mL extraction cells. The cells were extracted with the Dionex ASE200 system mentioned above using a chloroform/methanol mixture (2:1, v/v) at 120 °C and 1500 psi. The lipid content was determined gravimetrically after evaporation of the solvent. The extractable lipid content of each tissue or feces is summarized in Table S10.

Conjugate identification by liquid chromatography-tandem mass spectrometry (LC-MS/MS).

In order to further identify potential glucuronide and/or sulfate conjugates of hydroxylated PCB 91 metabolites in urine (Figure 1), a urine sample, filtered through a 0.45 µm filter, was analyzed on an Ascentis Express C₁₈ column (150 mm length, 3.0 mm inner diameter, 5 µm particle size; Supelco, St. Louis, MO) using an Agilent 1260 Infinity liquid chromatograph equipped with an Agilent 6460 MS/MS detector. The source parameters for the MS/MS detector were as follows: gas temp at 325 °C, gas flow at 10 L/min, nebulizer at 20 psi, sheath gas temp at 400 °C, sheath gas flow at 12 L/min, capillary negative at 3500 V. The mobile phases were 10 mM NH₄Ac in water (pH=6.8) and acetonitrile, with a flow rate at 0.3 mL/min. The concentration of acetonitrile in mobile phase increased from 30 % to 50 % from 5 to 30 min; increased to 85 % from 30 to 40 min; was maintained for 5 min, and finally decreased to 30 % from 45 to 50 min. The injection volume was 10 µL. MS electrospray in negative ionization mode was utilized. The presence of 5-91 and 4-91 were confirmed based on scan mode with a mass in the range of 100-800 amu and selective ion mode (SIM) with *m/z* 341 and retention time matched to authentic standards.

In order to detect unknown metabolites, such as glucuronides and sulfates, the theoretical isotope ratios of 0.617:1:0.648 and a SIM method with the following *m/z* were used to screen for metabolites: Dihydroxylated PCB 91 conjugated with a single sulfate moiety *m/z* at 434.82, 436.82, and 438.82; dihydroxylated PCB 91 conjugated with a single glucuronide moiety *m/z* at 530.89, 532.89, 534.89; hydroxylated PCB 91 conjugated with a sulfate moiety *m/z* at 418.8, 420.8, 422.8; and hydroxylated PCB 91 conjugated with a glucuronide moiety *m/z* at 514.9, 516.9, 518.9. The presence of glucuronide or sulfate metabolites of PCB 91 in urine was further confirmed in the multiple reaction monitoring (MRM) mode using transitions of *m/z* 516.9 > 175 for hydroxylated PCB 91 glucuronides and *m/z* 218.5 > 79 for dihydroxylated PCB 91 sulfates. Other transitions were not confirmed.

Statistical analyses.

All data are reported as mean \pm one standard deviation. Differences in levels and EF values between both genotypes were assessed using two-sample, two-tailed Student's t-test. Differences between EF values of the racemate and the samples were evaluated using two-sample, one-tailed Student's t-test. Differences were considered statistically significant for $p < 0.05$. Changes in the concentration of OH-PCB metabolites in the urine after β -glucuronidase/sulfatase treatment were assessed with interaction plots using R (Figures S1 to S3).⁴²

RESULTS

PCB 91 tissue and excreta levels.

PCB 91 levels in KO mice, expressed as %TD, followed the rank order adipose > liver > brain >> blood (Figure 2). The PCB 91 detected in these four tissues accounted for approximately 55 %TD (Table S6). When adjusted for tissue wet weight, PCB 91 levels in tissues from KO mice also decreased in the order adipose tissues ($190 \pm 60 \mu\text{g/g}$ wet weight) > liver ($44 \pm 17 \mu\text{g/g}$ wet weight) > brain ($2.8 \pm 1.0 \mu\text{g/g}$ wet weight) > blood ($0.32 \pm 0.12 \mu\text{g/g}$ wet weight) (Table S2). In WT mice, PCB 91 levels followed a similar rank order when PCB levels were expressed as %TD (Figure 2) or adjusted for tissue wet weight (Table S2). For example, PCB 91 levels, adjusted for tissue wet weight, decreased in the order adipose tissues ($92 \pm 88 \mu\text{g/g}$ wet weight) > liver ($1.8 \pm 0.8 \mu\text{g/g}$ wet weight) > brain ($0.57 \pm 0.40 \mu\text{g/g}$ wet weight) > blood ($0.09 \pm 0.05 \mu\text{g/g}$ wet weight) (Table S2). In contrast to KO mice, the PCB 91 residue in these tissues from WT mice accounted for only 20 %TD. Moreover, levels of PCB 91 were significantly higher in the blood, brain, liver, and excreta from KO compared to WT mice (Figure 2; Tables S2 and S6). PCB 91 levels in adipose tissue were also higher in the adipose tissue of KO compared to WT mice; however, this difference was not statistically significant, irrespective of how the PCB 91 levels were adjusted. It is noteworthy that the %TD of PCB 91 in the liver were 30-times higher in KO compared to WT mice, with 9 %TD and 0.3 %TB of PCB 91 being retained in the liver of KO and WT mice, respectively (Table S6).

The amount of PCB 91 excreted with the feces was one order of magnitude higher in KO (4 %TD) compared to WT mice (0.4 %TD) and decreased from day 1 to day 3. Levels of PCB 91 decreased from 3 %TD to 0.2 %TD in KO mice and from 0.3 %TD to 0.05 %TD in WT mice in this period (Figure 2. Table S6). The same trend was observed when PCB 91 levels were expressed in a tissue wet weight basis (Table S2). For example, PCB 91 levels were over one order of magnitude higher in feces collected on day 1 from KO compared to WT mice (8.4 ± 4.7 and $0.76 \pm 0.61 \mu\text{g/g}$ wet weight, respectively). It is noteworthy that despite the larger %TD of PCB 91 excreted with the feces in KO mice, the amount of PCB 91 retained in the liver was also much higher in KO compared to WT mice. This observation is consistent with impaired metabolism of PCB 91 in KO mice.

The amount of PCB 91 excreted with the urine was also higher in KO compared to WT mice (Figure 2). Briefly, KO mice excreted 4 %TD, and WT mice excreted 0.3 %TD with the urine over the three-day study period. In KO mice, the amount of PCB 91 in the urine

decreased from 2 %TD on day 1 to 0.8 %TD on day 3. Levels of PCB 91 decreased from 0.2 %TD on day 1 to 0.02 %TD on day 3 in the urine from WT mice. Similar trends were observed when PCB 91 levels were adjusted for tissue wet weight (Table S2).

Levels of OH-PCB 91 metabolites.

The disposition of OH-PCB metabolites of PCB 91 has not been investigated *in vivo* to-date. We, therefore, measured the levels of the OH-PCB 91 metabolites shown in Figure 1 in selected tissues and excreta. Four OH-PCB 91 metabolites, including 3–100 (2,2',4,4',6-pentachlorobiphenyl-3-ol), 5–91, 4–91 and 4,5–91, were detected in blood, liver, feces, and urine collected from both KO and WT mice (Figure 2; Table S6). 3–100, a minor metabolite, is formed via an arene oxide intermediate that undergoes a 1,2-chlorine shift to form a hydroxylated PCB 100 (2,2',4,4',6-pentachlorobiphenyl) metabolite.

5–91 was the major metabolites detected in blood, liver, feces, and urine, with 5–91 levels decreasing in the rank order feces > urine > liver > blood. Tissue levels of 5–91, adjusted for tissue wet weight, were similar in KO and WT mice. For example, levels of 5–91 were $1,200 \pm 1,300$ and $1,300 \pm 1,600$ ng/g wet weight in the liver of KO and WT mice, respectively (Table S3). Importantly, the sum of 5–91 in the four compartments investigated in this study accounted for approximately 23 %TD and 31 %TD in KO and WT mice, respectively (Table S6). In contrast, the sum of the minor metabolites, including 3–100, 4–91 and 4,5–91, in the same compartments represented only 1.1 %TD and 2.3 %TD in KO and WT mice, respectively. The levels of these minor metabolites in blood and liver ranged from 2 to 110 ng/g wet weight and, as discussed for 5–91 above, showed no statistically significant differences between KO and WT mice (Table S2).

Feces was the major and urine a minor route of excretion of OH-PCB 91 metabolites (Figure 3). In WT mice, the amount of 5–91 decreased from 17 %TD to 5 %TD in feces and 0.05 %TD to 0.01 %TD in urine from day 1 to day 3. In KO mice, the amount of 5–91 decreased from 12 %TD to 4 %TD in feces and 0.3 %TD to 0.07 %TD in the urine. Although more OH-PCBs in both excreta were generally lower in excreta from KO compared to WT mice, these differences did not reach statistical significance.

Preliminary characterization of urinary OH-PCB conjugates.

To assess the formation of phase II metabolites, aliquots of urine samples were incubated in parallel with and without a β -glucuronidase/sulfatase mixture. Levels of 5–91 and 4,5–91, but not 4–91 were higher in urine samples collected on day 1 to day 3 urines after deconjugation (Figure 4; Table S6, Figure S1–S3). These findings provide indirect evidence that OH-PCB metabolites of PCB 91 are metabolized to OH-PCB conjugates that are eliminated with the urine. LC-MS/MS was used to further screen for the presence of OH-PCB 91 metabolites and their conjugates in a representative urine sample. The hydroxylated metabolites of PCB 91 eluted with a retention time of ~42 min, as determined with authentic standards of 4–91 and 5–91. Consistent with our quantitative analysis (Figure 3; Table S6), 5–91 was a major and 4–91 a minor metabolite (Figures 4A and 4B). The other two OH-PCB 91 metabolites could not be identified because of the low levels of these metabolites in urine samples, and because no authentic hydroxylated standard was available.

Several OH-PCB 91 conjugates were detected at retention times < 20 min (Figures 4C and 4D). Two peaks with m/z 514.9, 516.9 and 518.9 in an isotope ratio matching the theoretical isotope ratio of a pentachlorinated compound (i.e., 0.617:1:000:648) were observed at retention times of 7.538 and 13.863 min. Both peaks were tentatively identified as OH-PCB 91 glucuronides (Figure 4D). Analysis in the MRM mode with a transition of m/z 516.8 > 175.0 further confirmed the identification of both metabolites as OH-PCB 91 glucuronides (Figure 4D). A peak of a pentachlorinated metabolite with m/z 434.82, 436.82, and 438.82 was observed at a retention time of 3.125 min (not shown). This peak corresponds to a dihydroxylated PCB 91 metabolite conjugated with a single sulfate moiety; however, we could not confirm the presence of this metabolite in the MRM mode.

Enantiomeric fractions of PCB 91.

Only limited information is available about the atropisomeric enrichment of PCB 91 in rodents. To address this knowledge gap, we investigated the genotype-dependent atropisomeric enrichment of PCB 91 in selected tissues and excreta of mice (Figure 5). The PCB 91 atropisomer eluting first on the BDM column (E_1 -PCB 91) was significantly enriched in adipose, blood, brain, and liver in both of KO and WT mice (Figure 5A; Table S7). The same PCB 91 atropisomer was enriched in the liver, and blood samples analyzed on the CD column, and the extent of the atropisomeric enrichment, determined using the EF values, was comparable for analyses on both columns (Table S7). EF values of PCB 91 ranged from 0.74 in adipose tissue to 0.94 in the liver of WT mice exposed to racemic PCB 91 (Table S7). A less pronounced atropisomeric enrichment was observed in tissues from KO mice, with EF values of PCB 91 ranging from 0.60 in adipose tissue to 0.69 in brain and liver. EF values of PCB 91 followed the rank order liver > brain ~ blood > adipose in WT mice, and liver ~ brain ~ blood > adipose in KO mice. E_1 -PCB 91 was also enriched in feces samples from all time points investigated. The EF values in feces increased from day 1 to day 3. In day 3 samples, the EF values of PCB 91 in feces were close to those observed in the liver (Table S7). Moreover, the extent of the atropisomeric enrichment of E_1 -PCB 91 in feces samples was less pronounced in KO compared to WT mice.

Enantiomeric fractions of OH-PCB 91 metabolites.

Atropselective analyses of 5-91 and 4-91 in blood and liver were performed in the BDM column (Figures 5B and 5C). Analyses on the CD column confirmed the extent and direction of the atropisomeric enrichment of 5-91 observed on the BDM column (Table S7). E_1 -5-91 was enriched in blood from both KO and WT mice, with more pronounced atropisomeric enrichment in WT compared to KO mice (Figure 5B). E_1 -5-91 was also enriched in the liver from WT mice, but the atropisomeric enrichment was less pronounced compared to blood. Near racemic chiral signature of 5-91 were observed in the liver of KO mice. A marked enrichment of E_1 -4-91 was observed in liver and blood from both KO and WT mice, and no significant differences in EF values were found by genotype (Figure 5C).

In contrast to the enrichment observed in tissues, E_2 -5-91 was enriched in feces from KO mice (Figure 5B). The atropisomeric enrichment of E_2 -5-91 became less pronounced from day 1 to day 3, resulting in a near racemic EF value of 0.45 on day 3 in KO mice. In WT mice, E_2 -5-91 was enriched in feces samples collected on day 1 after PCB exposure,

whereas E₁-5-91 was enriched in feces samples collected on day 2 and day 3. As a result, the EF values of 5-91 in feces samples were always significantly lower in KO mice than WT mice. E₂-5-91 was enriched considerably in urine samples from KO mice (all days) and WT mice (day 1 only) (Table S7). Similar to feces, EF values of 5-91 in urine samples also increased from day 1 to day 3 in both KO and WT mice, as determined on the CD column (Table S7). However, a more pronounced atropisomeric enrichment of E₂-5-91 was observed in KO compared to WT mice.

Consistent with the enrichment of E₁-4-91 in tissues, E₁-4-91 was enriched in feces samples collected on days 1 to 3. The extent of the enrichment of E₁-4-91 increased from day 1 to day 3. Similar EF values were observed in day 1 feces samples from KO and WT mice. Statistically significant differences in the EF values of KO compared to WT mice were found in day 2 and day 3 feces samples, with a more pronounced atropisomeric enrichment of E₁-4-91 being present in feces samples obtained from WT mice.

DISCUSSION

Disposition of PCB 91 in KO and WT mice.

In this disposition study, levels of PCB 91 were significantly higher in blood and tissues from female KO compared to age-matched congenic WT mice exposed orally to PCB 91. We observed a similar difference in the disposition of PCB 136 in tissues from KO and WT exposed to racemic PCB 136 using the same dosing paradigm.^{25, 43} In both studies, a considerable percentage of the total dose of both parent PCBs was accumulated in the liver of KO mice. The accumulation of PCBs, such as PCB 91, in the liver of KO, but not WT mice, is an indirect result of the liver-specific deletion of *crp*. Briefly, KO mice have an impaired metabolism of bile acids and lipids in the liver and, consequently, have livers with higher levels of extractable lipids and hepatic cytochrome P450 proteins compared to congenic WT mice.^{25, 30, 44, 45} Studies in rats demonstrate that fatty liver results in a redistribution of PCBs, such as PCB 126 (3,3',4,4',5-pentachlorobiphenyl), from the adipose tissue to the liver, potentially with higher levels of PCBs in the liver compared to adipose tissue.^{46, 47} Other lipophilic compounds also accumulate in the liver in models of non-alcoholic fatty liver disease.⁴⁸ Moreover, *ortho* chlorinated PCB congeners bind to hepatic cytochrome P450 enzymes⁴⁹ and, as a result, can be sequestered into the liver in the absence of hepatic metabolism. Similarly, dioxin-like PCB congeners (i.e., PCB 126) are retained in the rodent liver due to binding to CYP1A enzymes.^{50, 51} Together, the hepatic accumulation of PCB 91 and the impaired hepatic PCB metabolism result in changes in the toxicokinetics of PCB 91 in KO compared to WT mice that, as we described recently for PCB 136,⁴³ result in higher PCB levels in blood and tissues from KO mice at later time points (i.e., 72 h after PCB administration).

Feces is a route of elimination of PCBs, such as PCB 136, in mice^{25, 34-36} and rats.⁵² Typically, less than 2 % of the total dose is eliminated with the feces over a three-day period in C57Bl/6 mice exposed orally to PCBs.^{19, 29-31} Mice exposed by oral gavage to a PCB mixture, however, excreted > 10 %TD of PCB 91 within 12 h.⁵³ The excretion of a higher %TD of unresorbed PCBs in this earlier study is likely due to differences in the mouse strain and the mode of administration (cookie in this study vs. oral gavage in our earlier study⁵³).

In the present study, feces was also a route of excretion of PCB 91 in both KO and WT. Moreover, there were clear differences in the extent of fecal excretion between genotypes, with KO mice excreting 10-times more PCB 91 than WT mice based on the total PCB 91 dose. In contrast, only 5-times more PCB 136 was excreted with the feces in KO than WT mice (4.9 %TD vs. 0.95 %TD, respectively) following oral exposure to PCB 136.²⁵ Overall, the more pronounced fecal excretion of PCB 91 and PCB 136 in KO mice is due to the higher fat content of the feces of KO mice. The higher fecal fat content in KO mice has been reported previously and is the result of an impaired bile acid metabolism in KO mice caused by the liver-specific deletion of *cpr*, which in turn reduces the absorption of fats from the gastrointestinal tract.⁵⁴ The larger amount of non-resorbed fats in KO mice not only reduces the oral bioavailability of PCBs (*i.e.*, increases their elimination without absorption),⁵⁵ but also increases their elimination from the gastrointestinal tract (*i.e.*, their diffusion from the bloodstream into the gastrointestinal tract).⁵⁶ Our earlier PCB disposition study also demonstrated that a higher fecal fat content was associated with higher fecal PCB levels.⁵³

The present study revealed differences in the distribution of PCB 91 and PCB 136 in KO mice. We observed 60-fold higher levels of PCB 136,²⁵ but only 30-fold higher levels of PCB 91 in the liver of KO compared to WT mice. At the same time, much less PCB 136 was present in the liver of exposed KO mice (4.2 %TD of PCB 136 compared to 9 %TD of PCB 91). The differences in the hepatic accumulation of both PCB congeners are consistent with differences in the toxicokinetics of both congeners that, in turn, are the result of differences in their extrahepatic metabolism. To the best of our knowledge, no studies have investigated how an impaired hepatic metabolism, for example, due to mutations or deficiencies in CPR expression, or genetic polymorphisms of cytochrome P450 enzymes involved in the metabolism of PCBs (e.g., CYP2A6 and CYP2B6) alters the PCB profiles and levels in the human liver. It is also unknown how fatty liver affects the disposition of PCBs in humans. It seems likely that congener-specific differences in the distribution of PCBs in the normal versus diseased liver play an overlooked role in the progression of alcoholic or non-alcoholic fatty liver disease. For example, the activation of human nuclear transcription factors implicated in non-alcoholic fatty liver disease is complex and highly congener specific.⁵⁷ Thus, higher hepatic PCB levels are expected to alter the expression of drug metabolizing enzymes in an already diseased liver, a hypothesis that warrants further attention, especially considering the high global prevalence of alcoholic and non-alcoholic liver disease.⁵⁸

Disposition of OH-PCB 91 metabolites in KO and WT mice.

Although a large body of evidence demonstrates that PCB metabolites are toxic,^{5, 6} only limited information about the metabolism of structurally diverse PCB congeners, including PCB 91, is available. In the present study, hydroxylated metabolites of PCB 91 were present in blood, liver, and excreta of KO and WT mice. These observations are consistent with studies of the disposition of PCB 95 and PCB 136 in mice.^{37, 59} Levels of OH-PCBs were below the limit of detection in the adipose and brain tissue, irrespective of the genotype. In a separate study, we reported congener-dependent OH-PCBs profiles in the brain of neonatal mice and the corresponding dams exposed developmentally to racemic PCB 95 and PCB 136 via the maternal diet.¹⁵ OH-PCBs were also detected in the brain of wildlife (*i.e.*, cetaceans⁶⁰ and polar bears⁶¹) and rats.¹⁶ Feces was a major route of excretion of OH-PCB

91 metabolites. It is noteworthy that hydroxylated PCB 91 metabolites accounted for 24 %TD and 33 %TD of PCB 91 in the feces of KO and WT mice, respectively. Similarly, feces was a major and urine a minor route of excretion of hydroxylated metabolites of PCB 136 in mice.²⁵ In contrast, two lower chlorinated PCB congeners, PCB 3 and PCB 11 were rapidly eliminated as metabolites with both the urine and feces in rats exposed by inhalation to the respective PCB congener.⁶²⁻⁶⁴

The distribution of OH-PCB metabolites revealed differences compared to our previous study with PCB 136 in the same mouse model.²⁵ Briefly, 2,2',3,3',6,6'-hexachlorobiphenyl-5-ol (5-136) accounted for 26 %TD of PCB 136 in WT mice in the earlier study, whereas the structurally related 5-91 accounted for 31 %TD of PCB 91 in this study. In KO mice, both *meta* hydroxylated metabolites accounted for a comparable %TD in the blood, liver, feces, and urine (i.e., 24 %TD of PCB 136 vs. 23 %TD PCB 91). The %TD of 2,2',3,3',6,6'-hexachlorobiphenyl-4-ol (4-136), a *para* hydroxylated metabolite, was 4.6-times and 3.9-time higher compared to the %TD of the structurally analogous 4-91 in KO and WT mice, respectively. Unlike our previous study with PCB 136,²⁵ we observed no statistically significant differences in the tissue levels of PCB 91 metabolite between WT and KO mice. In contrast, liver and blood levels of OH-PCB 136 metabolites were typically significantly higher in KO compared to WT mice after oral exposure to PCB 136.²⁵ *In vitro* metabolism studies with precision-cut liver tissue slices also demonstrate congener-specific differences in the metabolism of PCBs, with PCB 91 being more rapidly oxidized in *meta*, but not *para* position compared to PCB 136. These differences in the metabolism of PCB 91 and PCB 136 may be toxicologically important because, depending on their substitution pattern, OH-PCBs display different toxicities.^{5, 6}

OH-PCBs are further metabolized to glucuronide and sulfate metabolites in rodent models^{52, 62, 65} and humans.⁶⁶ Because conjugates of OH-PCBs are potential biomarkers of PCB exposure,⁶³ we screened urine samples for the presence of OH-PCB 91 conjugates. Only 5-91 and 4,5-91 conjugates were excreted with the urine based on our deconjugation experiments. Similarly, 5-136 and 2,2',3,3',6,6'-hexachlorobiphenyl-4,5-diol (4,5-136), but not 4-136 were excreted with the urine as OH-PCB 136 conjugates following exposure of WT and KO mice PCB 136.²⁵ Our screening of a representative urine sample by LC-MS/MS for metabolites identified an OH-PCB 91 glucuronide. Besides, we observed a dihydroxylated PCB 91 metabolite conjugated with a single sulfate moiety; however, we could not confirm the presence of this metabolite in the MRM mode. The detection of these metabolites in urine is not entirely unexpected. For examples, several studies have shown the presence of mono- and dihydroxylated PCB conjugates in urine for rats exposed to lower chlorinated PCBs.^{62, 63, 67} A recent study reported complex PCB metabolite profiles, including dihydroxylated PCB metabolites conjugated with a single sulfate moiety, in serum from polar bears and feces from mice exposed to a complex PCB mixture.⁶⁸ Further accurate mass determinations and MS/MS experiments are therefore warranted to confirm the formation of these OH-PCB 91 metabolites and study their disposition in mice.

Atropisomeric enrichment of PCB 91 and its OH-PCB metabolites.

Chiral PCBs, such as PCB 91, are atropselectively oxidized by cytochrome P450 enzymes, resulting in an atropisomeric enrichment of both the parent PCB and its hydroxylated metabolites.^{1, 26} Moreover, several studies reveal differences in the hepatotoxicity and neurotoxicity of pure PCB atropisomers.²⁶ For example, PCB 91 causes atropselective metabolic and lipidomic responses in earthworms *in vivo*.⁶⁹ Based on the elution order of PCB 91 atropisomers on the BDM column, the enrichment of E₁-PCB 91 in mice was consistent with *in vitro* studies with mouse liver tissue slices⁴⁰ and disposition studies in mice exposed orally to a PCB mixture containing PCB 91.^{53, 70} E₁-PCB 91 was also enriched in studies with recombinant rat CYP2B1 and rat liver microsomes^{41, 71, 72} and human liver microsomes.²⁰ Similarly, fish species, seabirds and ringed seals typically showed enrichment of E₁-PCB 91.^{73, 74} An enrichment of E₂-PCB 91 was reported only in a few seabirds and human breastmilk samples.⁷⁵ Unlike PCB 91, the direction of the atropisomeric enrichment of several toxicologically relevant PCB congeners, in particular, PCB 95 and PCB 136, is different in mice compared to other mammalian species. For example, *in vitro*, and *in vivo* studies demonstrate that (-)-PCB 136 is more rapidly eliminated in mice. In contrast, (+)-PCB 136 is more rapidly metabolized in other mammalian species, resulting in an enrichment of (-)-PCB 136.¹

The enrichment of PCB 91 in this study was genotype-dependent, with a more pronounced atropisomeric enrichment observed in WT compared to KO mice. This difference in the atropisomeric enrichment is consistent in the slower metabolism of PCB 91 in KO compared to WT mice. In contrast, we did not observe significant differences in the EF values in tissues from KO and WT mice in our earlier disposition studies with PCB 136 at the 48 and 72 h time points,^{25, 43} an observation that further highlights the congener-specific differences in the disposition of PCBs (i.e., PCB 91 vs. PCB 136) in KO mice discussed above. The higher fat content in the liver of KO mice does not directly contribute to different EF values in WT compared to KO mice because the partitioning of PCB into fatty tissues is a physicochemical process that is not atropselective. However, the storage of a significant percentage of the total dose of PCB 91 in the liver of KO mice will distribute the PCB away from the site of metabolism and contribute to a reduced elimination of PCB 91, which in turn will influence the atropisomeric enrichment of PCB 91 in target tissues and affect toxic outcomes.

The two major PCB 91 metabolites, 5-91 and 4-91, were formed with significant atropisomeric enrichment in KO and WT mice. Typically, the E₁-atropisomers of 5-91 and 4-91 displayed enrichment in the compartments investigated, irrespective of the genotype. The enrichment of E₂-5-91 in day 1 feces samples from WT mice and day 1 and day 2 feces samples from KO was a notable exception. In contrast, E₂-5-91 and E₂-4-91 are preferentially formed in studies with mouse liver tissue slices.⁴⁰ These findings demonstrate that *in vitro* metabolism studies do not necessarily predict the atropisomeric enrichment of OH-PCB *in vivo*. This observation is not entirely surprising because *in vitro* models do not recapitulate the complex metabolism and transport processes present *in vivo*, including the metabolism of PCB metabolites by the intestinal microbiome. It is likely that further metabolism of OH-PCBs to the corresponding sulfates and glucuronides as well as the

transport of these PCB metabolites is atropselective, thus resulting in complex chiral mixtures of the OH-PCBs. Consistent with this interpretation of our results; we observed the presence of conjugated PCB 91 metabolites in urine. Moreover, the altered direction of the enrichment of the atropisomers of 5–91 in day 1 compared to day 2 and day 3 samples in WT mice could be due to the atropselective phase II metabolism or transport of OH-PCB 91 metabolites. Further studies of the atropselective metabolism of OH-PCBs to sulfate, glucuronide and other conjugates are needed to confirm this hypothesis.

Overall, our study demonstrates differences in the atropselective disposition of PCB 91 and its hydroxylated metabolites in KO compared to WT mice. Moreover, there are congener-specific difference in the disposition of PCB 91 compared to our earlier study with PCB 136. These differences in the disposition of PCB and their metabolites are not only due to the impaired hepatic metabolism of PCBs caused by the lack of *cpr* expression in the liver, but also the accumulation of the parent PCB in the liver. Because the deletion of *cpr* in the liver does not appear to alter the neurodevelopment in KO compared to WT mice, KO mice are a model that could be used to study how an altered disposition of chiral PCBs and OH-PCBs affects neurotoxic outcomes. However, it will be challenging to determine how impaired PCB metabolism vs. PCB sequestration in the fatty liver contribute to toxic outcomes. Moreover, there are significant differences in the atropselective metabolism of PCBs in mice and humans.¹⁹ Humanized mouse models, such as mice expressing human CYP2B6 enzymes in the liver,⁷⁶ are alternatives for studies of the role of PCB metabolism in PCB-induced developmental neurotoxicity and other adverse outcomes associated with exposure to PCBs.

Supplementary Material

Refer to Web version on PubMed Central for supplementary material.

ACKNOWLEDGMENTS

The authors thank Dr. Xinxin Ding of the Wadsworth Center, New York State Department of Health, for providing the mouse model, Dr. E. Davis Oldham for help with the animal work, Austin Kammerer for help with the PCB analysis, Dr. Kai Wang for advice regarding the statistical analysis, and Dr. Izabela Kania-Korwel for technical support and a critical review of the manuscript.

FUNDING SOURCES

This work was supported by grants ES027169, ES013661, and ES005605 from the National Institute of Environmental Health Sciences, National Institutes of Health. The content is solely the responsibility of the authors and does not necessarily represent the official views of the National Institute of Environmental Health Sciences or the National Institutes of Health.

Abbreviations:

%TD	percent of the total PCB 91 dose
3–100	2,2',4,4',6-pentachlorobiphenyl-3-ol
4'–159	2,3,3',4,5,5'-hexachlorobiphenyl-4'-ol
4,5–136	2,2',3,3',6,6'-hexachlorobiphenyl-4,5-diol

4,5-91	2,2',3,4',6-pentachlorobiphenyl-4,5-diol
4-136	2,2',3,3',6,6'-hexachlorobiphenyl-4-ol
4-91	2,2',3,4',6-pentachlorobiphenyl-4-ol
5-136	2,2',3,3',6,6'-hexachlorobiphenyl-5-ol
5-91	2,2',3,4',6-pentachlorobiphenyl-5-ol
BDM	ChiralDex BDM column
CD	CP-Chirasil-DEX CB column
CPR	cytochrome P450 reductase
E₁	atropisomer eluting first on the enantioselective capillary column
E₂	atropisomer eluting first on the enantioselective capillary column
EF	enantiomeric fraction
GC	gas chromatography
KO	mice with liver-specific deletion of the cytochrome P450 oxidoreductase gene
LC-MS/MS	liquid chromatography-tandem mass spectrometry
LOD	limit of detection
MRM	multiple reaction monitoring
OH-PCB	hydroxylated PCB metabolite
μECD	micro electron capture detector
PCB	polychlorinated biphenyl
PCB 100	2,2',4,4',6-pentachlorobiphenyl
PCB 117	2,3,4',5,6-pentachlorobiphenyl
PCB 126	3,3',4,4',5-pentachlorobiphenyl
PCB 136	2,2',3,3',6,6'-hexachlorobiphenyl
PCB 204	2,2',3,4,4',5,6,6'-octachlorobiphenyl
PCB 91	2,2',3,4',6-pentachlorobiphenyl
PCB 95	2,2',3,5',6-pentachlorobiphenyl
RyR	ryanodine receptor
SD	standard deviation

SIM	selective ion mode
WT	wild type mice

REFERENCES

1. Kania-Korwel I; Lehmler HJ, Chiral polychlorinated biphenyls: absorption, metabolism and excretion-a review. *Environ. Sci. Pollut. Res. Int* 2016, 23, 2042–2057. [PubMed: 25651810]
2. Hu D; Hornbuckle KC, Inadvertent polychlorinated biphenyls in commercial paint pigments. *Environ. Sci. Technol* 2010, 44, 2822–2827. [PubMed: 19957996]
3. Anezaki K; Nakano T, Concentration levels and congener profiles of polychlorinated biphenyls, pentachlorobenzene, and hexachlorobenzene in commercial pigments. *Environ. Sci. Poll. Res* 2013, 21, 1–12.
4. Herkert NJ; Jahnke JC; Hornbuckle KC, Emissions of tetrachlorobiphenyls (PCBs 47, 51, and 68) from polymer resin on kitchen cabinets as a non-Aroclor source to residential air. *Environ. Sci. Technol* 2018, 52, 5154–5160. [PubMed: 29667399]
5. Grimm FA; Hu D; Kania-Korwel I; Lehmler HJ; Ludewig G; Hornbuckle KC; Duffel MW; Bergman A; Robertson LW, Metabolism and metabolites of polychlorinated biphenyls. *Crit. Rev. Toxicol* 2015, 45, 245–272. [PubMed: 25629923]
6. Dhakal K; Gadupudi GS; Lehmler HJ; Ludewig G; Duffel MW; Robertson LW, Sources and toxicities of phenolic polychlorinated biphenyls (OH-PCBs). *Environ. Sci. Pollut. Res. Int* 2018, 25, 16277–16290. [PubMed: 28744683]
7. ATSDR Toxicological Profile for Polychlorinated Biphenyls (PCBs) <https://www.atsdr.cdc.gov/toxprofiles/tp.asp?id=142&tid=26> (accessed June 3, 2019).
8. Holland EB; Feng W; Zheng J; Dong Y; Li X; Lehmler H-J; Pessah IN, An extended structure-activity relationship of non-dioxin-like PCBs evaluates and supports modeling predictions and identifies picomolar potency of PCB 202 towards ryanodine receptors. *Toxicol. Sci* 2016, 155, 170–181. [PubMed: 27655348]
9. Niknam Y; Feng W; Cherednichenko G; Dong Y; Joshi SN; Vyas SM; Lehmler H-J; Pessah IN, Structure-activity relationship of select meta- and para-hydroxylated non-dioxin-like polychlorinated biphenyls: from single RyR1 channels to muscle dysfunction. *Toxicol. Sci* 2013, 136, 500–513. [PubMed: 24014653]
10. Pessah IN; Cherednichenko G; Lein PJ, Minding the calcium store: Ryanodine receptor activation as a convergent mechanism of PCB toxicity. *Pharmacol. Ther* 2010, 125, 260–285. [PubMed: 19931307]
11. Pessah IN; Lein PJ; Seegal RF; Sagiv SK, Neurotoxicity of polychlorinated biphenyls and related organohalogenes. *Acta Neuropathol* 2019, doi: 10.1007/s00401-00019-01978-00401.
12. Fonnum F; Mariussen E, Mechanisms involved in the neurotoxic effects of environmental toxicants such as polychlorinated biphenyls and brominated flame retardants. *J. Neurochem* 2009, 111, 1327–1347. [PubMed: 19818104]
13. Sethi S; Morgan RK; Peng W; Lin YP; Li XS; Luna C; Koch M; Bansal R; Duffel MW; Puschner B; Zoeller RT; Lehmler HJ; Pessah IN; Lein PJ, Comparative analyses of the 12 most abundant PCB congeners detected in human maternal serum for activity at the thyroid hormone receptor and ryanodine receptor. *Environ. Sci. Technol* 2019, 53, 3948–3958. [PubMed: 30821444]
14. Pessah IN; Hansen LG; Albertson TE; Garner CE; Ta TA; Do Z; Kim KH; Wong PW, Structure-activity relationship for noncoplanar polychlorinated biphenyl congeners toward the ryanodine receptor-Ca²⁺ channel complex type 1 (RyR1). *Chem. Res. Toxicol* 2006, 19, 92–101. [PubMed: 16411661]
15. Kania-Korwel I; Lukasiewicz T; Barnhart CD; Stamou M; Chung H; Kelly KM; Bandiera S; Lein PJ; Lehmler H-J, Congener-specific disposition of chiral polychlorinated biphenyls in lactating mice and their offspring: Implications for PCB developmental neurotoxicity. *Toxicol. Sci* 2017, 158, 101–115. [PubMed: 28431184]
16. Meerts IA; Assink Y; Cenijn PH; Van Den Berg JH; Weijers BM; Bergman A; Koeman JH; Brouwer A, Placental transfer of a hydroxylated polychlorinated biphenyl and effects on fetal and

- maternal thyroid hormone homeostasis in the rat. *Toxicol. Sci* 2002, 68, 361–371. [PubMed: 12151632]
17. Lesmana R; Shimokawa N; Takatsuru Y; Iwasaki T; Koibuchi N, Lactational exposure to hydroxylated polychlorinated biphenyl (OH-PCB 106) causes hyperactivity in male rat pups by aberrant increase in dopamine and its receptor. *Environ. Toxicol* 2014, 29, 876–883. [PubMed: 22996836]
 18. Meerts IATM; Lilienthal H; Hoving S; van den Berg JHJ; Weijers BM; Bergman A; Koeman JH; Brouwer A, Developmental exposure to 4-hydroxy-2,3,3',4',5-pentachlorobiphenyl (4-OH-CB107): Long-term effects on brain development, behavior, and brain stem auditory evoked potentials in rats. *Toxicol. Sci* 2004, 82, 207–218. [PubMed: 15310863]
 19. Uwimana E; Ruiz P; Li X; Lehmler HJ, Human CYP2A6, CYP2B6, and CYP2E1 atropselectively metabolize polychlorinated biphenyls to hydroxylated metabolites. *Environ. Sci. Technol* 2019, 53, 2114–2123. [PubMed: 30576102]
 20. Uwimana E; Li X; Lehmler H-J, Human liver microsomes atropselectively metabolize 2,2',3,4',6-pentachlorobiphenyl (PCB 91) to a 1,2-shift product as the major metabolite. *Environ. Sci. Technol* 2018, 52, 6000–6008. [PubMed: 29659268]
 21. Uwimana E; Li X; Lehmler H-J, 2,2',3,5',6-Pentachlorobiphenyl (PCB 95) is atropselectively metabolized to para-hydroxylated metabolites by human liver microsomes. *Chem. Res. Toxicol* 2016, 29, 2108–2110. [PubMed: 27989147]
 22. Wu X; Kammerer A; Lehmler HJ, Microsomal oxidation of 2,2',3,3',6,6'-hexachlorobiphenyl (PCB 136) results in species-dependent chiral signatures of the hydroxylated metabolites. *Environ. Sci. Technol* 2014, 48, 2436–2444. [PubMed: 24467194]
 23. Schnellmann RG; Putnam CW; Sipes IG, Metabolism of 2,2',3,3',6,6'-hexachlorobiphenyl and 2,2',4,4',5,5'-hexachlorobiphenyl by human hepatic microsomes. *Biochem. Pharmacol* 1983, 32, 3233–3239. [PubMed: 6416258]
 24. Lehmler HJ, Synthesis of environmentally relevant fluorinated surfactants--a review. *Chemosphere* 2005, 58, 1471–1496. [PubMed: 15694468]
 25. Wu X; Barnhart C; Lein PJ; Lehmler HJ, Hepatic metabolism affects the atropselective disposition of 2,2',3,3',6,6'-hexachlorobiphenyl (PCB 136) in mice. *Environ. Sci. Technol* 2015, 49, 616–625. [PubMed: 25420130]
 26. Lehmler H-J; Harrad SJ; Huhnerfuss H; Kania-Korwel I; Lee CM; Lu Z; Wong CS, Chiral polychlorinated biphenyl transport, metabolism, and distribution: A review. *Environ. Sci. Technol* 2010, 44, 2757–2766. [PubMed: 20384371]
 27. Pessah IN; Lehmler H-J; Robertson LW; Perez CF; Cabrales E; Bose DD; Feng W, Enantiomeric specificity of (–)-2,2',3,3',6,6'-hexachlorobiphenyl toward ryanodine receptor types 1 and 2. *Chem. Res. Toxicol* 2009, 22, 201–207. [PubMed: 18954145]
 28. Feng W; Zheng J; Robin G; Dong Y; Ichikawa M; Inoue Y; Mori T; Nakano T; Pessah IN, Enantioselectivity of 2,2',3,5',6-pentachlorobiphenyl (PCB 95) atropisomers toward ryanodine receptors (RyRs) and their influences on hippocampal neuronal networks. *Environ. Sci. Technol* 2017, 51, 14406–14416. [PubMed: 29131945]
 29. Yang D; Kania-Korwel I; Ghogha A; Chen H; Stamou M; Bose DD; Pessah IN; Lehmler HJ; Lein PJ, PCB 136 atropselectively alters morphometric and functional parameters of neuronal connectivity in cultured rat hippocampal neurons via ryanodine receptor-dependent mechanisms. *Toxicol. Sci* 2014, 138, 379–392. [PubMed: 24385416]
 30. Gu J; Weng Y; Zhang QY; Cui H; Behr M; Wu L; Yang W; Zhang L; Ding X, Liver-specific deletion of the NADPH-cytochrome P450 reductase gene: impact on plasma cholesterol homeostasis and the function and regulation of microsomal cytochrome P450 and heme oxygenase. *J. Biol. Chem* 2003, 278, 25895–25901. [PubMed: 12697746]
 31. Wu L; Gu J; Weng Y; Kluetzman K; Swiatek P; Behr M; Zhang QY; Zhuo X; Xie Q; Ding X, Conditional knockout of the mouse NADPH-cytochrome P450 reductase gene. *Genesis* 2003, 36, 177–181. [PubMed: 12929087]
 32. Joshi SN; Vyas SM; Duffel MW; Parkin S; Lehmler H-J, Synthesis of sterically hindered polychlorinated biphenyl derivatives. *Synthesis* 2011, 1045–1054. [PubMed: 21516177]

33. Kania-Korwel I; Shaikh NS; Hornbuckle KC; Robertson LW; Lehmler H-J, Enantioselective disposition of PCB 136 (2,2',3,3',6,6'-hexachlorobiphenyl) in C57BL/6 mice after oral and intraperitoneal administration. *Chirality* 2007, 19, 56–66. [PubMed: 17089340]
34. Kania-Korwel I; Hornbuckle KC; Robertson LW; Lehmler H-J, Dose-dependent enantiomeric enrichment of 2,2',3,3',6,6'-hexachlorobiphenyl in female mice. *Environ. Toxicol. Chem* 2008, 27, 299–305. [PubMed: 18348647]
35. Kania-Korwel I; Hornbuckle KC; Robertson LW; Lehmler H-J, Influence of dietary fat on the enantioselective disposition of 2,2',3,3',6,6'-hexachlorobiphenyl (PCB 136) in female mice. *Food Chem. Toxicol* 2008, 46, 637–644. [PubMed: 17950514]
36. Kania-Korwel I; Xie W; Hornbuckle KC; Robertson LW; Lehmler H-J, Enantiomeric enrichment of 2,2',3,3',6,6'-hexachlorobiphenyl (PCB 136) in mice after induction of CYP enzymes. *Arch. Environ. Contam. Toxicol* 2008, 55, 510–517. [PubMed: 18437444]
37. Kania-Korwel I; Barnhart CD; Stamou M; Truong KM; El-Komy MH; Lein PJ; Veng-Pedersen P; Lehmler H-J, 2,2',3,5',6-Pentachlorobiphenyl (PCB 95) and its hydroxylated metabolites are enantiomerically enriched in female mice. *Environ. Sci. Technol* 2012, 46, 11393–11401. [PubMed: 22974126]
38. Kania-Korwel I; Zhao H; Norstrom K; Li X; Hornbuckle KC; Lehmler H-J, Simultaneous extraction and clean-up of PCBs and their metabolites from small tissue samples using pressurized liquid extraction. *J. Chromatogr. A* 2008, 1214, 37–46. [PubMed: 19019378]
39. Wu X; Kania-Korwel I; Chen H; Stamou M; Dammanahalli KJ; Duffel M; Lein PJ; Lehmler H-J, Metabolism of 2,2',3,3',6,6'-hexachlorobiphenyl (PCB 136) atropisomers in tissue slices from phenobarbital or dexamethasone-induced rats is sex-dependent. *Xenobiotica* 2013, 43, 933–947. [PubMed: 23581876]
40. Wu X; Duffel M; Lehmler H-J, Oxidation of polychlorinated biphenyls by liver tissue slices from phenobarbital-pretreated mice is congener-specific and atropselective. *Chem. Res. Toxicol* 2013, 26, 1642–1651. [PubMed: 24107130]
41. Kania-Korwel I; Lehmler H-J, Assigning atropisomer elution orders using atropisomerically enriched polychlorinated biphenyl fractions generated by microsomal metabolism. *J. Chromatogr. A* 2013, 1278, 133–144. [PubMed: 23347976]
42. R Core Team (2013). R: A language and environment for statistical computing. R Foundation for Statistical Computing, Vienna, Austria URL <http://www.R-project.org/> (accessed June 3, 2019).
43. Li X; Wu X; Kelly KM; Veng-Pedersen P; Lehmler H-J, Toxicokinetics of chiral PCB 136 and its hydroxylated metabolites in mice with a liver-specific deletion of cytochrome P450 reductase. *Chem. Res. Toxicol* 2019, 32, 727–736. [PubMed: 30729780]
44. Gu J; Cui H; Behr M; Zhang L; Zhang Q-Y; Yang W; Hinson JA; Ding X, In vivo mechanisms of tissue-selective drug toxicity: effects of liver-specific knockout of the NADPH-cytochrome P450 reductase gene on acetaminophen toxicity in kidney, lung, and nasal mucosa. *Mol. Pharmacol* 2005, 67, 623–630. [PubMed: 15550675]
45. Wu L; Gu J; Cui H; Zhang QY; Behr M; Fang C; Weng Y; Kluetzman K; Swiatek PJ; Yang W; Kaminsky L; Ding X, Transgenic mice with a hypomorphic NADPH-cytochrome P450 reductase gene: effects on development, reproduction, and microsomal cytochrome P450. *J. Pharmacol. Exp. Ther* 2005, 312, 35–43. [PubMed: 15328377]
46. Van Birgelen APJM; Van der Kolk J; Fase KM; Bol I; Poiger H; Brouwer A; Van den Berg M, Toxic potency of 3,3',4,4',5-pentachlorobiphenyl relative to and in combination with 2,3,7,8-tetrachlorodibenzo-p-dioxin in a subchronic feeding study in the rat. *Toxicol. Appl. Pharmacol* 1994, 127, 209–221. [PubMed: 8048064]
47. Chu I; Villeneuve DC; Yagminas A; Lecavalier P; Poon R; Feeley M; Kennedy SW; Seegal RF; Hakansson H; Ahlborg UG; Valli VE, Subchronic toxicity of 3,3',4,4',5-pentachlorobiphenyl in the rat. I. Clinical, biochemical, hematological, and histopathological changes. *Fundam. Appl. Toxicol* 1994, 22, 457–468. [PubMed: 8050640]
48. Cichocki JA; Furuya S; Konganti K; Luo Y-S; McDonald TJ; Iwata Y; Chiu WA; Threadgill DW; Pogribny IP; Rusyn I, Impact of Nonalcoholic fatty liver disease on toxicokinetics of tetrachloroethylene in mice. *J. Pharmacol. Exp. Ther* 2017, 361, 17–28. [PubMed: 28148637]

49. Kania-Korwel I; Hrycay EG; Bandiera SM; Lehmler H-J, 2,2',3,3',6,6'-Hexachlorobiphenyl (PCB 136) atropisomers interact enantioselectively with hepatic microsomal cytochrome P450 enzymes. *Chem. Res. Toxicol* 2008, 21, 1295–1303. [PubMed: 18494506]
50. Chen JJ; Chen GS; Bunce NJ, Inhibition of CYP 1A2-dependent MROD activity in rat liver microsomes: An explanation of the hepatic sequestration of a limited subset of halogenated aromatic hydrocarbons. *Environ. Toxicol* 2003, 18, 115–119. [PubMed: 12635099]
51. Diliberto JJ; Burgin DE; Birnbaum LS, Effects of CYP1A2 on disposition of 2,3,7,8-tetrachlorodibenzo-p-dioxin, 2,3,4,7,8-pentachlorodibenzofuran, and 2,2',4,4',5,5'-hexachlorobiphenyl in CYP1A2 knockout and parental (C57BL/6N and 129/Sv) strains of mice. *Toxicol. Appl. Pharmacol* 1999, 159, 52–64. [PubMed: 10448125]
52. Birnbaum LS, Distribution and excretion of 2,3,6,2',3',6'- and 2,4,5,2',4',5'-hexachlorobiphenyl in senescent rats. *Toxicol. Appl. Pharmacol* 1983, 70, 262–272. [PubMed: 6414105]
53. Milanowski B; Lulek J; Lehmler H-J; Kania-Korwel I, Assessment of the disposition of chiral polychlorinated biphenyls in female mdr 1a/b knockout versus wild-type mice using multivariate analyses. *Environ. Int* 2010, 36, 884–892. [PubMed: 19923000]
54. Weng Y; DiRusso CC; Reilly AA; Black PN; Ding X, Hepatic gene expression changes in mouse models with liver-specific deletion or global suppression of the NADPH-cytochrome P450 reductase gene. Mechanistic implications for the regulation of microsomal cytochrome P450 and the fatty liver phenotype. *J. Biol. Chem* 2005, 280, 31686–31698. [PubMed: 16006652]
55. Gobas FAPC; Muir DCG; Mackay D, Dynamics of dietary bioaccumulation and fecal elimination of hydrophobic organic chemicals in fish. *Chemosphere* 1988, 17, 943–962.
56. Redgrave TG; Wallace P; Jandacek RJ; Tso P, Treatment with a dietary fat substitute decreased Arochlor 1254 contamination in an obese diabetic male. *J. Nutr. Biochem* 2005, 16, 383–384. [PubMed: 15936651]
57. Wahlang B; Falkner KC; Clair HB; Al-Eryani L; Prough RA; States JC; Coslo DM; Omiecinski CJ; Cave MC, Human receptor activation by Arochlor 1260, a polychlorinated biphenyl mixture. *Toxicol. Sci* 2014, 140, 283–297. [PubMed: 24812009]
58. Younossi Z; Anstee QM; Marietti M; Hardy T; Henry L; Eslam M; George J; Bugianesi E, Global burden of NAFLD and NASH: trends, predictions, risk factors and prevention. *Nat. Rev. Gastroenterol. Hepatol* 2017, 15, 11–20. [PubMed: 28930295]
59. Kania-Korwel I; Barnhart CD; Lein PJ; Lehmler H-J, Effect of pregnancy on the disposition of 2,2',3,5',6-pentachlorobiphenyl (PCB 95) atropisomers and their hydroxylated metabolites in female mice. *Chem. Res. Toxicol* 2015, 28, 1774–1783. [PubMed: 26271003]
60. Kunisue T; Sakiyama T; Yamada TK; Takahashi S; Tanabe S, Occurrence of hydroxylated polychlorinated biphenyls in the brain of cetaceans stranded along the Japanese coast. *Mar. Pollut. Bull* 2007, 54, 963–973. [PubMed: 17445835]
61. Gebbink WA; Sonne C; Dietz R; Kirkegaard M; Riget FF; Born EW; Muir DC; Letcher RJ, Tissue-specific congener composition of organohalogen and metabolite contaminants in East Greenland polar bears (*Ursus maritimus*). *Environ. Pollut* 2008, 152, 621–629. [PubMed: 17707109]
62. Dhakal K; Uwimana E; Adamcakova-Dodd A; Thorne PS; Lehmler HJ; Robertson LW, Disposition of phenolic and sulfated metabolites after inhalation exposure to 4-chlorobiphenyl (PCB3) in female rats. *Chem. Res. Toxicol* 2014, 27, 1411–1420. [PubMed: 24988477]
63. Dhakal K; Adamcakova-Dodd A; Lehmler HJ; Thorne PS; Robertson LW, Sulfate conjugates are urinary markers of inhalation exposure to 4-chlorobiphenyl (PCB3). *Chem. Res. Toxicol* 2013, 26, 853–855. [PubMed: 23713983]
64. Hu X; Adamcakova-Dodd A; Thorne PS, The fate of inhaled ¹⁴C-labeled PCB11 and its metabolites in vivo. *Environ. Int* 2014, 63, 92–100. [PubMed: 24275706]
65. Lucier GW; McDaniel OS; Schiller CM; Matthews HB, Structural requirements for the accumulation of chlorinated biphenyl metabolites in the fetal rat intestine. *Drug Metab. Dispos* 1978, 6, 584–590. [PubMed: 30609]
66. Grimm FA; Lehmler HJ; Koh WX; DeWall J; Teesch LM; Hornbuckle KC; Thorne PS; Robertson LW; Duffel MW, Identification of a sulfate metabolite of PCB 11 in human serum. *Environ. Int* 2017, 98, 120–128. [PubMed: 27816204]

67. Dhakal K; He X; Lehmler H-J; Teesch LM; Duffel MW; Robertson LW, Identification of sulfated metabolites of 4-chlorobiphenyl (PCB3) in the serum and urine of male rats. *Chem. Res. Toxicol* 2012, 25, 2796–2804. [PubMed: 23137097]
68. Liu Y; Richardson ES; Derocher AE; Lunn NJ; Lehmler HJ; Li X; Zhang Y; Cui JY; Cheng L; Martin JW, Hundreds of unrecognized halogenated contaminants discovered in polar bear serum. *Angew. Chem. Int. Ed.* 2018, 57, 16401–16406. [PubMed: 30376612]
69. He Z; Wang Y; Zhang Y; Cheng H; Liu X, Stereoselective bioaccumulation of chiral PCB 91 in earthworm and its metabolomic and lipidomic responses. *Environ. Poll* 2018, 238, 421–430.
70. Kania-Korwel I; El-Komy MHME; Veng-Pedersen P; Lehmler H-J, Clearance of polychlorinated biphenyl atropisomers is enantioselective in female C57Bl/6 mice. *Environ. Sci. Technol* 2010, 44, 2828–2835. [PubMed: 20384376]
71. Kania-Korwel I; Duffel MW; Lehmler H-J, Gas chromatographic analysis with chiral cyclodextrin phases reveals the enantioselective formation of hydroxylated polychlorinated biphenyls by rat liver microsomes. *Environ. Sci. Technol* 2011, 45, 9590–9596. [PubMed: 21966948]
72. Lu Z; Kania-Korwel I; Lehmler HJ; Wong CS, Stereoselective formation of mono- and dihydroxylated polychlorinated biphenyls by rat cytochrome P450 2B1. *Environ. Sci. Technol* 2013, 47, 12184–12192. [PubMed: 24060104]
73. Wong CS; Mabury SA; Whittle DM; Backus SM; Teixeira C; DeVault DS; Bronte CR; Muir DCG, Organochlorine compounds in Lake Superior: Chiral polychlorinated biphenyls and biotransformation in the aquatic food web. *Environ. Sci. Technol* 2004, 38, 84–92. [PubMed: 14740721]
74. Warner NA; Norstrom RJ; Wong CS; Fisk AT, Enantiomeric fractions of chiral polychlorinated biphenyls provide insights on biotransformation capacity of arctic biota. *Environ. Toxicol. Chem* 2005, 24, 2763–2767. [PubMed: 16398111]
75. Bordajandi LR; Abad E; Gonzalez MJ, Occurrence of PCBs, PCDD/Fs, PBDEs and DDTs in Spanish breast milk: Enantiomeric fraction of chiral PCBs. *Chemosphere* 2008, 70, 567–575. [PubMed: 17727913]
76. Zhang QY; Gu J; Su T; Cui H; Zhang XL; D'Agostino J; Zhuo XL; Yang WZ; Swiatek PJ; Ding XX, Generation and characterization of a transgenic mouse model with hepatic expression of human CYP2A6. *Biochem. Biophys. Res. Commun* 2005, 338, 318–324. [PubMed: 16126166]

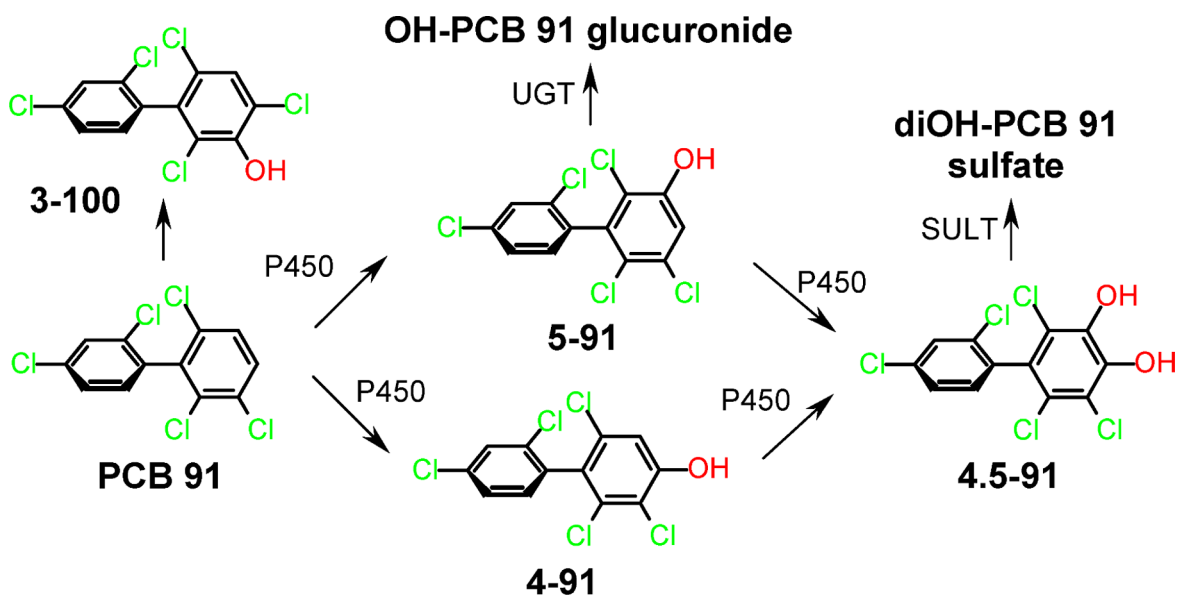


Figure 1:
Simplified metabolism scheme of PCB 91. Only one atropisomer of PCB 91 and its metabolites are shown for clarity reasons. 4-91, 2,2',3,4',6-pentachlorobiphenyl-4-ol; 5-91, 2,2',3,4',6-pentachlorobiphenyl-5-ol; 4,5-91, 4,5-dihydroxy-2,2',3,4',6-pentachlorobiphenyl; 3-100, 2,2',4,4',6-pentachlorobiphenyl-3-ol; PCB 91, 2,2',3,4',6-pentachlorobiphenyl; P450, cytochrome P450 enzyme; SULT, sulfotransferase; and UGT, uridine 5'-diphospho-glucuronosyltransferase.

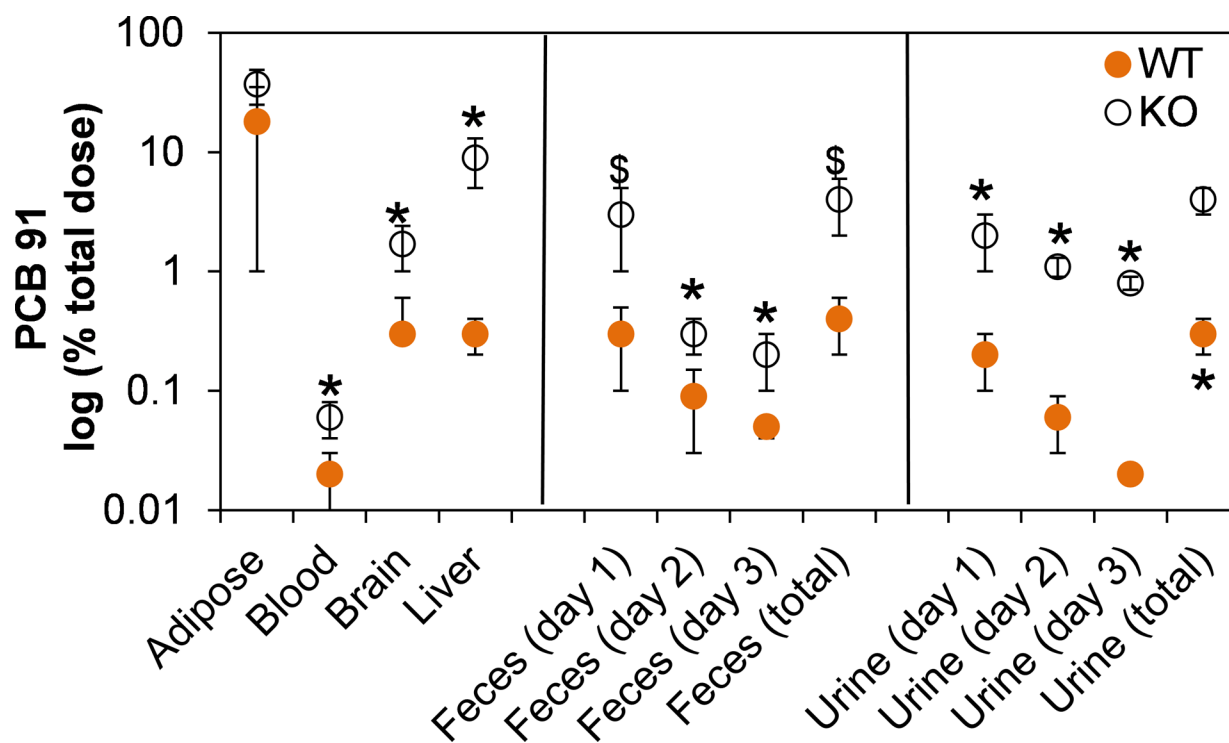
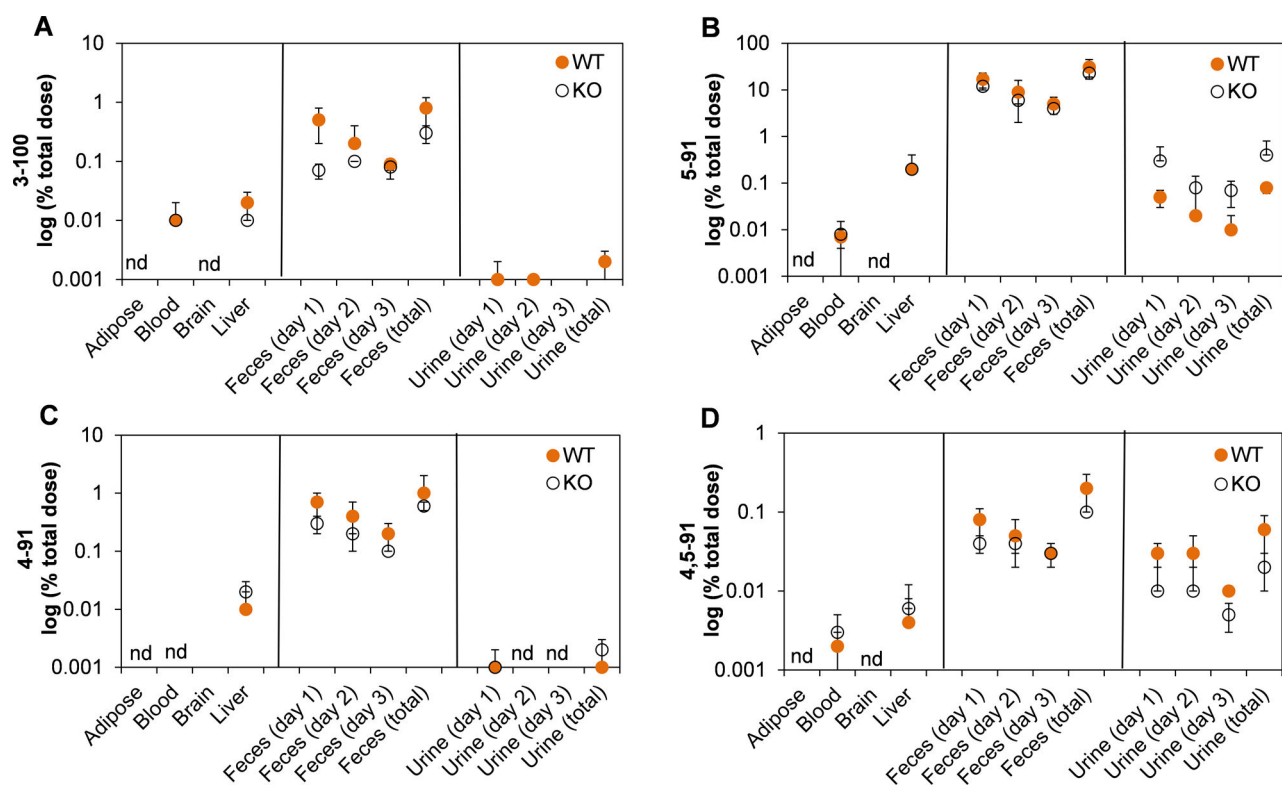


Figure 2.

Mice with a liver-specific deletion of the *cpr* gene (KO mice) have significantly higher levels of PCB 91 compared to the corresponding congenic wild type mice (WT mice). PCB 91 levels are expressed on a logarithmic scale as a percent of the total PCB 91 dose (see Table S6 for additional details). *Significantly different from WT ($p < 0.05$) analyzed by Student's t-test; \$ ($0.05 < p < 0.1$) analyzed by Student's t-test; nd, not detected.

**Figure 3.**

Levels of (A) 3–100, (B) 5–91, (C) 4–91, (D) 4,5–91 in tissues and excreta show no statistically significant differences between mice with a liver-specific deletion of the *cpr* gene (KO mice) and the corresponding congenic wild type mice (WT mice). OH-PCB metabolite levels are expressed on a logarithmic scale as a percent of the total PCB 91 dose (see Table S6 for additional details). nd, not detected.

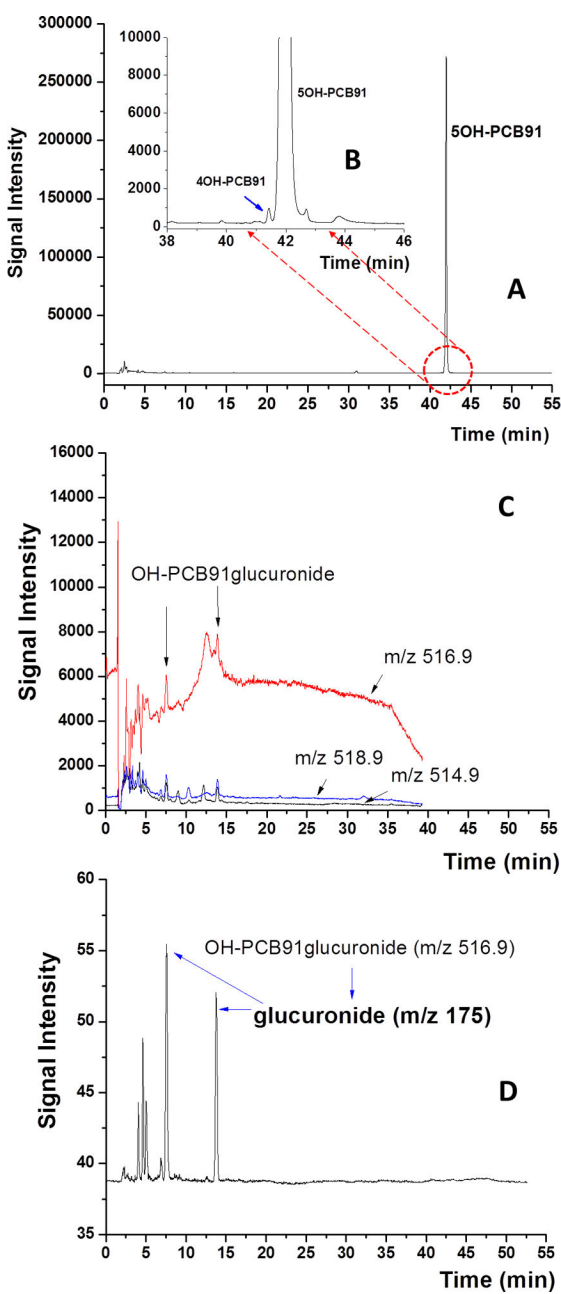


Figure 4:

Analysis of a urine sample from a representative mouse dosed with PCB 91 by LC/MS demonstrates the presence of PCB 91 metabolites. The presence of (A) 5–91 and (B) 4–91 was confirmed in the scan mode with a mass in the range of 100–800 amu in the negative mode. (C) Analysis in the SIM mode showed two peaks at retention times of 7.5 and 13.9 min. Their isotope ratios at m/z 514.9, 516.9, and 518.9 matched the theoretical ratio of 0.617:1:0.648, which is consistent with the presence of OH-PCB 91 glucuronides in the urine sample. (D) Analysis in the MRM mode showed two peaks with transitions of m/z 516.9 > 175.0 at the same retention times, further confirming the presence of OH-PCB 91 glucuronides. The instrument parameters are described in the Experimental section.

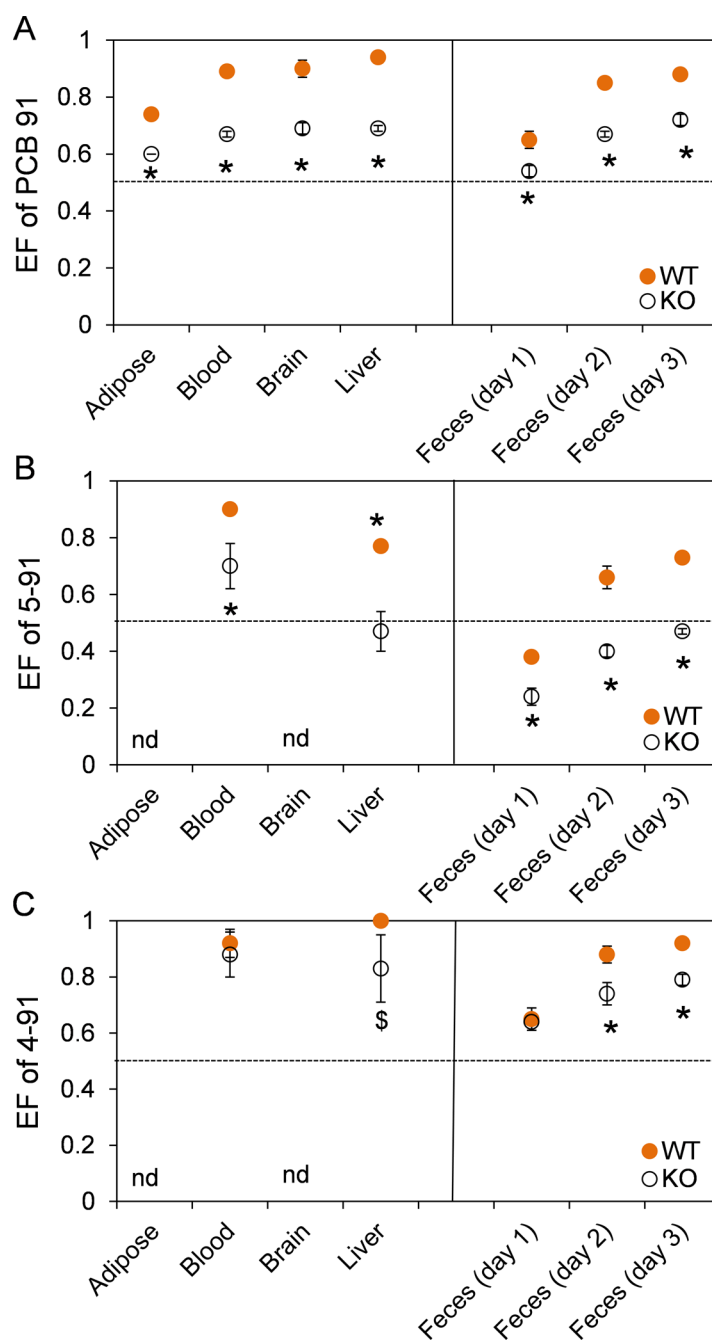


Figure 5. Comparison of the enantiomeric fractions (EFs) of (A) PCB 91, (B) 5-91 and (C) 4-91 in tissues and feces reveals significant differences in the atropisomeric enrichment between KO and WT mice following oral administration of PCB 91. EF values greater than 0.5 represent an enrichment of the first eluting atropisomer (E_1), and EF values less than 0.5 represent an enrichment of the second eluting atropisomer (E_2). Atropselective separations were performed on a BDM column as described in the Experimental section. The dotted line

indicates the EF values of the respective racemic standard. * Significantly different from WT ($p < 0.05$) analyzed by Student's t-test; $^{\$} p < 0.1$ analyzed by Student's t-test; nd, not detected.

Author Manuscript

Author Manuscript

Author Manuscript

Author Manuscript